

# Coexisting ferro- and antiferromagnetism in Ni<sub>2</sub>MnAl Heusler alloys

Mehmet Acet,<sup>a)</sup> Eyup Duman, and Eberhard F. Wassermann

*Tiefemperaturphysik, Gerhard-Mercator Universität Duisburg, D-47048 Duisburg, Germany*

Lluís Mañosa and Antoni Planes

*Department d'Estructura i Constituents de la Matèria, Facultat de Física, Universitat de Barcelona, Diagonal 647, 08028 Barcelona, Catalonia, Spain*

(Received 3 June 2002; accepted for publication 11 July 2002)

The structural and magnetic properties of stoichiometric Ni<sub>2</sub>MnAl are studied to clarify the conditions for ferromagnetic and antiferromagnetic ordering claimed to occur in this compound. X-ray and magnetization measurements show that although a single phase *B2* structure can be stabilized at room temperature, a single *L2*<sub>1</sub> phase is not readily stabilized, but rather a mixed *L2*<sub>1</sub>+*B2* state occurs. The mixed state incorporates ferromagnetic and antiferromagnetic parts for which close-lying Curie and a Néel temperatures can be identified from magnetization measurements. © 2002 American Institute of Physics. [DOI: 10.1063/1.1504498]

## I. INTRODUCTION

Among the Heusler compounds, Ni<sub>2</sub>MnGa and Ni<sub>2</sub>MnAl undergo martensitic transformations at compositions around stoichiometric, with the transformation temperature *M*<sub>s</sub> varying rapidly with small changes in the concentration of the constituents.<sup>1–3</sup> Ni<sub>2</sub>MnGa is ferromagnetic in both the parent *L2*<sub>1</sub> and the product martensitic phase,<sup>4</sup> and it has been demonstrated that in the martensitic phase, strains on the order of 10% can be induced in single crystals by applying an external magnetic field of about 1 T leading to the magnetic shape memory effect.<sup>5</sup> Obviously, this property provides a technological value for Ni<sub>2</sub>MnGa, and a great deal of effort has been invested in research to understand the properties of the martensitic phase in this alloy.<sup>6–11</sup>

Stoichiometric Ni<sub>2</sub>MnAl is structurally stable down to the lowest temperatures, but martensitic transformations occur in the slightly off-stoichiometric compounds, and their mechanical properties are more favorable than those of the relatively brittle Ni<sub>2</sub>MnGa. It is, therefore, thought that Ni<sub>2</sub>MnAl could be provided as an alternative material if its magnetic shape memory properties are as favorable as those of Ni<sub>2</sub>MnGa. However, the magnetic state of Ni<sub>2</sub>MnAl has been an issue that has not been adequately clarified, and whether a single *L2*<sub>1</sub> parent phase that is not mixed with the *B2* phase can be stabilized is still controversial. The pure *B2* phase in Ni<sub>2</sub>MnAl can be retained by annealing at 950 K and subsequently quenching to room temperature. On the other hand, it appears that it is difficult to produce a single *L2*<sub>1</sub> phase, since the *B2*–*L2*<sub>1</sub> transformation in this compound requires long term annealing at about 650 K where the diffusion kinetics are relatively slow as compared to the faster kinetics at 1000 K where Ni<sub>2</sub>MnGa can be annealed to readily stabilize the *L2*<sub>1</sub> phase.

The magnetic ordering in the retained metastable *B2* phase of Ni<sub>2</sub>MnAl is conical antiferromagnetic.<sup>12</sup> In the *L2*<sub>1</sub>

phase, there is some indirect evidence based on calorimetric measurements that the magnetic ordering is ferromagnetic.<sup>13</sup> Although no direct evidence has been reported on either the ferromagnetic nature of the *L2*<sub>1</sub> parent phase or the martensitic product phase of off-stoichiometric Ni<sub>2</sub>MnAl, it has been possible to induce considerable strain on a single crystal specimen which has, however, not exceeded about 0.2%.<sup>14</sup> This appears to be a problem of not having a single *L2*<sub>1</sub> parent phase in the sample. If it were possible to increase the amount of *L2*<sub>1</sub> in an *L2*<sub>1</sub>+*B2* mixed phase, the strain in the martensitic state would also increase. This is a point that certainly requires further investigation. However, to be able to give a thorough account on the properties of structural phase transitions and magnetic shape memory effects in off-stoichiometric Ni<sub>2</sub>MnAl alloys, it is necessary, first, to understand the magnetic properties of the relatively simpler stoichiometric Ni<sub>2</sub>MnAl compound in the *B2* and *L2*<sub>1</sub> phases.<sup>15</sup> This makes up the theme of the present article, in which we investigate the structural and magnetic properties by x-ray diffraction, magnetization, magnetic susceptibility, and specific heat measurements.

## II. EXPERIMENT

The sample with stoichiometric composition was prepared by induction melting in a water cooled Cu crucible. The concentration of the sample was determined by energy dispersive x ray analysis to be 50.4 at. % Ni, 24.7 at. % Mn, and 24.9 at. % Al. To stabilize the *B2* phase, the sample was annealed at *T*<sub>a</sub>=923 K for 30 days and subsequently quenched in water to room temperature. The *L2*<sub>1</sub> phase was prepared by annealing a separate sample at *T*<sub>a</sub>=653 K for 30 days cut from the same ingot. The structure was examined by x-ray diffraction on the polycrystalline samples. Susceptibility measurements were carried out in a field-cooled (FC) and zero-FC (ZFC) sequence using a superconducting quantum interference device magnetometer in the temperature range 4 K ≤ *T* ≤ 400 K and using a vibrating sample magnetometer in the temperature range 300 K ≤ *T* ≤ 600 K. *M* versus *B* mea-

<sup>a)</sup> Author to whom correspondence should be addressed; electronic mail: acet@tphysik.uni-duisburg.de

measurements were carried out in fields up to 5 T. The specific heat was measured in the interval  $200\text{ K} \leq T \leq 500\text{ K}$  in a modulated differential scanning calorimeter with a temperature modulation of 0.5 K with a period of 80 s and a heating and cooling rate of 2 K/min.

### III. RESULTS

#### A. X-ray measurements

For both samples, the results of the x-ray measurements in the interval  $30^\circ \leq 2\theta \leq 60^\circ$  and  $60^\circ \leq 2\theta \leq 90^\circ$  are shown in Figs. 1(a) and 1(b), respectively. The locations of the expected reflection peaks are indicated by the arrows. Because of texturing in the polycrystalline specimen, the relative intensities are not in proportion, and some reflections are absent such as the (111) reflection for the sample with  $T_a = 923\text{ K}$ . The broad character of the peaks for  $T_a = 653\text{ K}$  indicates that this temperature is not sufficient to remove the strains. The strains are relaxed when annealed at  $T_a = 923\text{ K}$  as seen by the relatively narrower line shapes in the data for this annealing temperature.

For  $T_a = 923\text{ K}$ , only peaks associated with the  $B2$  phase are found, whereas for  $T_a = 653\text{ K}$ , the (331) peak related to the  $L2_1$  phase emerges as seen in Fig. 1(b). Less obvious is the emergence of a peak at the position of the (311) reflection in Fig. 1(a). The  $L2_1$  phase is certainly present, but it cannot be concluded from these data whether the phase is single phase or mixed with  $B2$ . The lattice constant of the  $B2$  phase is estimated to be  $a = 0.2909\text{ nm}$ , half that of the  $L2_1$  phase with  $a = 0.5818\text{ nm}$ , which is in agreement with earlier reported values.<sup>12</sup>

#### B. The magnetization and susceptibility

The magnetic field dependence of the magnetization  $M(B)$  and the temperature dependence of the magnetic susceptibility  $\chi(T)$  of the two samples are shown in Figs. 2–5.  $\chi(T)$  was measured first in the ZFC state followed by the measurement in the FC state. Prior to each  $M(B)$  measurement, the samples were prepared in the ZFC state by bringing them above 350 K. In the following, the samples are referred to by their annealing temperatures.

##### 1. Magnetization and susceptibility of the $T_a = 923\text{ K}$ sample

For the sample prepared in the  $B2$  phase, the  $M$  versus  $B$  curves up to 5 T in Fig. 2 have no substantial curvature, indicating that ferromagnetic coupling is not present or very weak in the case where there are traces of ferromagnetic inhomogeneities.

$\chi(T)$  in FC and ZFC states shown in Fig. 3 exhibits a peak at about 313 K. This temperature coincides with the Néel temperature  $T_N$  given as the onset of conical antiferromagnetic ordering previously reported for this system.<sup>12</sup> Therefore, referring back to Fig. 2, it becomes clear that the nearly linear behavior of the  $M$  versus  $B$  curves is due to the antiferromagnetism. Below  $T_N$ , the susceptibility decreases with decreasing temperature and increases again below about 130 K in both modes of measurement. Since the magnetization curves at 5 and 150 K in Fig. 2 appear not to be much

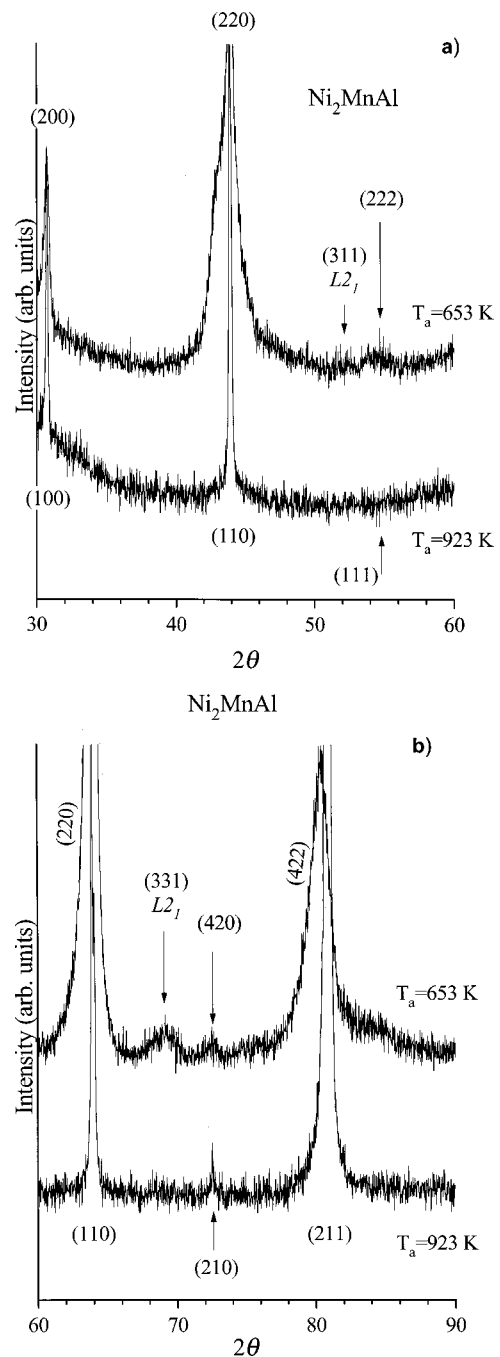


FIG. 1. The x-ray spectrum of  $\text{Ni}_2\text{MnAl}$ : (a) for  $30^\circ \leq 2\theta \leq 60^\circ$  and (b) for  $60^\circ \leq 2\theta \leq 90^\circ$  under both annealing conditions. (331) peak in part (b) is the indication for the presence of the  $L2_1$  phase. The (311) position in part (a), which would also be associated with the  $L2_1$  phase, is also indicated.

different from one another, the rise in  $\chi(T)$  below 130 K cannot be associated with some partial ferromagnetic ordering. It is not possible to give a detailed account for this behavior from the susceptibility data alone, but this property could be related to a reorientation of the conical structure which is frequently encountered in compounds incorporating Mn.

Another dominant feature in Fig. 3 is the splitting between the FC and the ZFC data below  $T_N$ . Such a splitting that occurs just below a magnetic transition temperature is usually an indication of different configurational “pinning”

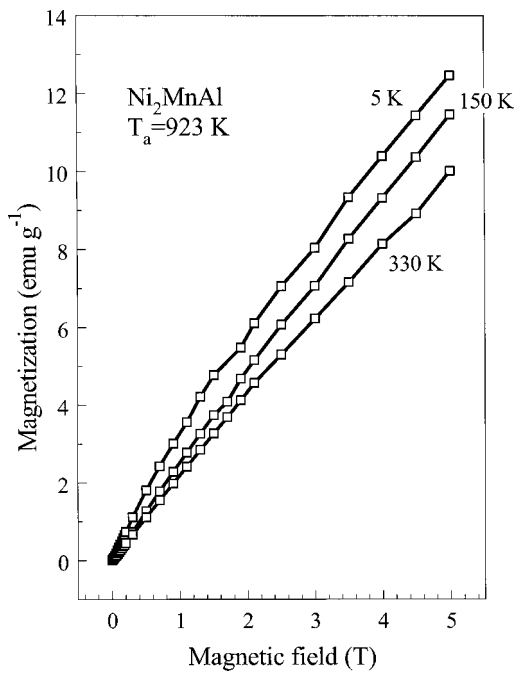


FIG. 2. The magnetic field dependence of the magnetization for the sample with  $T_a=923$  K. There is no appreciable curvature at any of the temperatures.

of residual or intrinsic ferromagnetic parts by the antiferromagnetic environment depending on whether the sample is brought into a FC or a ZFC state.<sup>16</sup> This property is discussed in more detail in Sec. IV.

**2. Magnetization and susceptibility of the  $T_a=653$  K sample**

As seen in Fig. 4, the  $M$  versus  $B$  curves of this sample have substantial curvature between 5 and 340 K as compared

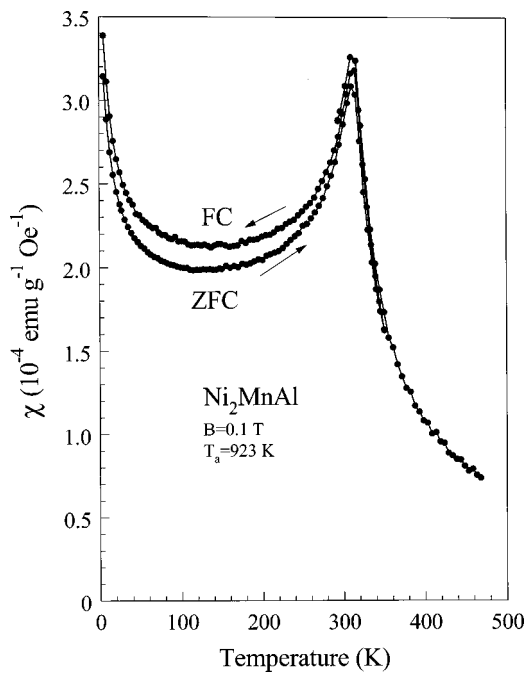


FIG. 3. The temperature dependence of the FC and ZFC magnetic susceptibility of  $Ni_2MnAl$  for  $T_a=923$  K. The peak at 313 K corresponds to  $T_N$ .

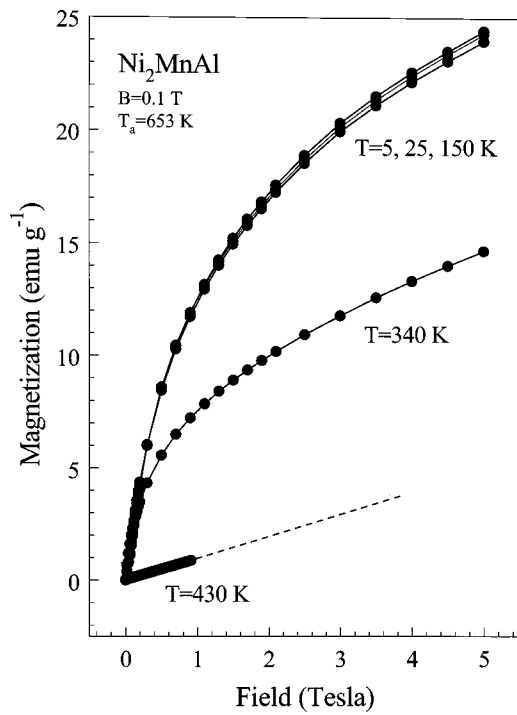


FIG. 4. The magnetic field dependence of the magnetization for the sample with  $T_a=653$  K. The curvature, indicating the presence of ferromagnetic exchange, is no longer present at 430 K. The dashed line is only a guide for the linear magnetic field dependence of the 430 K data below 1 T.

to the curves in Fig. 2, but they do not saturate even at the highest fields.  $M$  versus  $B$  becomes linear first above 400 K where the sample is paramagnetic (the maximum field in the vibrating sample magnetometer is 1 T). These data indicate

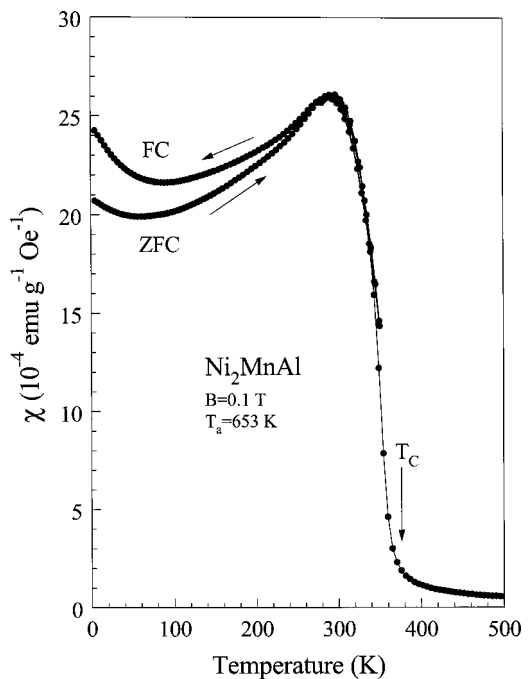


FIG. 5. The temperature dependence of the FC and ZFC magnetic susceptibility of  $Ni_2MnAl$  for  $T_a=653$  K.  $T_C$  is at about 375 K. The rounded peak results from the close lying temperatures corresponding to  $T_N$  and the temperature at which the magnetization of the ferromagnetic parts begin to saturate with decreasing temperature.

that annealing at  $T_a = 653$  K generates ferromagnetism and, evidently, the ferromagnetic entity is then the  $L2_1$  phase. However, the fact that  $M$  versus  $B$  does not saturate implies that a nonferromagnetic entity is also present. According to x-ray data, this entity can only be the antiferromagnetism of the  $B2$  phase. Therefore, even after 30 days of annealing at 653 K, the sample cannot be brought into a single  $L2_1$  phase.

The mixed nature of this state can be further evidenced from  $\chi(T)$  in Fig. 5 when the features are compared to those of  $\chi(T)$  in Fig. 3. The features of the two curves appear similar at first. In Fig. 5, a peak in  $\chi(T)$  is present at 293 K, which is somewhat lower than the temperature corresponding to the peak in Fig. 3. A splitting is present below the temperature corresponding to this peak, and  $\chi(T)$  runs through a minimum at lower temperatures. However, the value of  $\chi$  in Fig. 5 is about an order of magnitude greater and, furthermore, the approach from high temperatures to the maximum in  $\chi(T)$  shows a ferromagnetic-like behavior. The Curie temperature  $T_C$  is estimated to be about 375 K from this figure, which is close to the temperature where an anomaly was observed in previous differential scanning calorimetry measurements on an off-stoichiometric compound.<sup>13</sup> However, the fact that  $\chi(T)$  decreases below 293 K indicates that antiferromagnetism is simultaneously present in this state of the sample. The feature in the curve close to  $T_N$  is somewhat rounded out and is not as sharp as in Fig. 3 due to the close neighboring of  $T_N$  and the temperature of about 300 K at which the magnetization of the ferromagnetic contribution begins to level out as the temperature decreases.

Also, in Fig. 5, a splitting between the FC and ZFC susceptibilities occurs as the temperature decreases as in the data of Fig. 3. The magnitude of the splitting is larger than that in Fig. 3, because of the larger number of ferromagnetic parts in the sample in the  $L2_1+B2$  phase as compared to that in the sample in the  $B2$  state.  $\chi(T)$  increases with decreasing temperature below 90 K in the FC case and below 75 K in the ZFC case. The cause is expected to be related to the same effect giving rise to the minimum in  $\chi(T)$  of the  $B2$  phase sample.

### C. Specific heat

The specific heat  $c_p(T)$  of the samples with the two different heat treatments is shown in Fig. 6.  $c_p(T)$  of  $Ni_2MnGa$  measured in the same calorimeter is also shown for comparison.<sup>10</sup>  $c_p(T)$  of  $Ni_2MnAl$  in the  $B2$  state reaches a peak value at about  $T_{max} = 305$  K, which is somewhat lower than  $T_N = 313$  K determined from  $\chi(T)$ . The structure of the curve around the maximum is not as sharp as the peak at  $T_C = 390$  K of the ferromagnetic compound  $Ni_2MnGa$ .

$c_p(T)$  of the sample in the  $L2_1+B2$  state has a broad shoulder centered around  $T_{max} = 350$  K, and the narrower feature seen in the peak in the data of the  $B2$  sample is lost. The Curie temperature of the  $L2_1$  phase determined from the  $\chi(T)$  data lies closer to the minimum observed at 380 K. The mixed nature of the state produced by annealing at  $T_a = 653$  K is reflected in  $c_p(T)$  as well, whereby the close lying  $T_N$  and  $T_C$  of the  $L2_1+B2$  phase leads to an overlap of

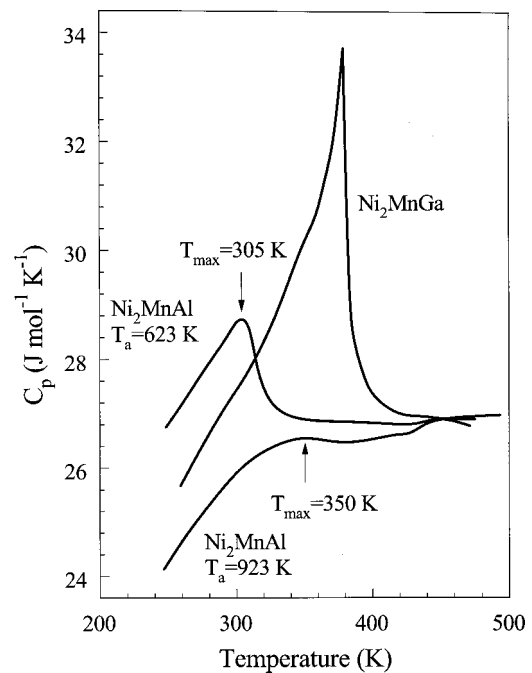


FIG. 6. The temperature dependence of the specific heat of  $Ni_2MnAl$  under both annealing conditions. That of  $Ni_2MnGa$  is shown for comparison.

the features in the data of both magnetic states that causes any sharp details at the transitions to be smeared out.

## IV. DISCUSSION

With the present magnetization measurements, we give evidence that the  $L2_1$  phase of  $Ni_2MnAl$  is ferromagnetic.  $T_C$  determined from  $\chi(T)$  data is found to be nearly the same as that of  $Ni_2MnGa$ . This is understandable, since the valence electron concentration  $e/a$  of both compounds is the same, and it is known that for  $Ni_2MnGa$   $T_C$  varies systematically and very slowly with  $e/a$ .<sup>4</sup>  $T_C$  of the  $L2_1$  phase of  $Ni_2MnAl$  also agrees well with the temperature corresponding to the anomaly occurring in calorimetric studies on an off-stoichiometric compound.<sup>13</sup> The nature of the magnetic coupling in  $Ni_2MnAl$  appears to be governed essentially by the Mn–Mn distance as in many other ordered compounds incorporating a sufficiently high concentration of Mn. At large separations the compounds are ferromagnetic and at small separations they tend to be antiferromagnetic. This is a tendency that is also found in the results of band calculations on Heusler alloys.<sup>6,17</sup> The shortest distance between Mn atoms in the  $L2_1$  phase of  $Ni_2MnAl$  is 0.411 nm. The  $B2$  phase occurs when Mn and Al atoms are arranged randomly, and the shortest Mn–Mn distance can then become 0.291 nm.

The  $B2$  to  $L2_1$  transformation in  $Ni_2MnAl$  occurs at a temperature where diffusion kinetics in a solid are slow. This enables the high temperature  $B2$  phase to be readily retained at room temperature as a metastable state rather than the thermodynamically more favorable  $L2_1$  phase. The development of the  $L2_1$  phase on annealing just below the temperatures of the transformation boundary does not produce a single  $L2_1$  phase in  $Ni_2MnAl$  in a period of 30 days, because either this time is too short or a metastable equilibrium be-

tween the  $B2$  and the  $L2_1$  phase is reached. The amount of  $L2_1$  can certainly depend on the metallurgical state of the sample. However, this must be checked by examining the field dependence of the magnetization on samples prepared with different grain sizes and internal strain. For  $\text{Ni}_2\text{MnAl}$ , the field dependence of the magnetization can give strong evidence as to whether the sample is a single phase  $B2$  or  $L2_1$ , or mixed.

In magnetically heterogeneous systems where ferromagnetism and antiferromagnetism coexist in the form of granular precipitates or in the form of independent long range ordered entities, a divergence of the FC and ZFC susceptibilities is encountered at the lower magnetic transition temperature be it  $T_C$  or  $T_N$ .<sup>16</sup> The only condition is that the external field should be sufficiently small, otherwise the effect can be lost or the point of divergence will shift to low temperatures. When a sample is cooled from  $T_N > T > T_C$  to below  $T_C$ , or from  $T_C > T > T_N$  to below  $T_N$  in finite or zero magnetic field, the spins become pinned in different configurations by the antiferromagnetic anisotropy. Therefore, the FC–ZFC mode of measurement in small fields becomes useful when it comes to deciding whether different forms of long range magnetic structures coexist. If  $\text{Ni}_2\text{MnAl}$  in the  $B2$  phase were a collinear antiferromagnet, no splitting between the FC and ZFC modes would be observed. Therefore, in this sample, there is either some residual  $L2_1$  phase, which provides the ferromagnetic exchange, or the conical antiferromagnetic structure of the  $B2$  phase has a ferromagnetic component. Both can give rise to pinning.

Despite the metallurgical problems of obtaining a single  $L2_1$  phase, off-stoichiometric  $\text{Ni}_2\text{MnAl}$  remains as a potential candidate for a magnetic shape memory material if this problem can be overcome. A further problem is to be able to give a clear picture on the magnetism of the martensitic

phase of the alloys. Although there have been some useful attempts to provide an understanding of the magnetic states in such alloys,<sup>18</sup> the details of the magnetic interactions remain to be clarified.

## ACKNOWLEDGMENTS

The authors acknowledge gratefully the support provided by IBERDROLA and CICYT (Project No. MAT2001-002351).

- <sup>1</sup>V. A. Chernenko, E. Cesari, V. V. Kokorin, and I. N. Vitenko, *Scr. Metall. Mater.* **33**, 1239 (1995).
- <sup>2</sup>R. Kainuma, H. Nakano, and K. Ishida, *Metall. Mater. Trans. A* **27A**, 4153 (1996).
- <sup>3</sup>S. Morito and K. Otsuka, *Mater. Sci. Eng., A* **208**, 47 (1996).
- <sup>4</sup>V. A. Chernenko, *Scr. Mater.* **40**, 523 (1999).
- <sup>5</sup>A. Sozinov, A. A. Likhachev, N. Lanska, and K. Ullako, *Appl. Phys. Lett.* **80**, 1746 (2002).
- <sup>6</sup>A. Ayuela, J. Enkovaara, K. Ulakko, and R. M. Nieminen, *J. Phys.: Condens. Matter* **11**, 2017 (1999).
- <sup>7</sup>R. Tickle, R. D. James, T. Shield, M. Wuttig, and V. V. Kokorin, *IEEE Trans. Magn.* **35**, 4302 (1999).
- <sup>8</sup>R. Tickle and R. D. James, *J. Magn. Magn. Mater.* **195**, 627 (1999).
- <sup>9</sup>Ll. Mañosa and A. Planes, *Adv. Solid State Phys.* **40**, 361 (2000).
- <sup>10</sup>Ll. Mañosa, A. González-Comas, E. Obrad'o, A. Planes, V. A. Chernenko, V. V. Kokorin, and E. Cesari, *Phys. Rev. B* **55**, 11068 (1997).
- <sup>11</sup>T. Castán, E. Vives, and P. Lindgård, *Phys. Rev. B* **60**, 7071 (1999).
- <sup>12</sup>K. R. A. Ziebeck and P. J. Webster, *J. Phys. F: Met. Phys.* **5**, 1756 (1975).
- <sup>13</sup>F. Gejima, Y. Sutou, R. Kainuma, and K. Ishida, *Metall. Mater. Trans. A* **30A**, 2721 (1999).
- <sup>14</sup>A. Fujita, K. Fukamichi, F. Gejima, R. Kainuma, and K. Ishida, *Appl. Phys. Lett.* **77**, 3054 (2000).
- <sup>15</sup>El. Mañosa, A. Planes, Ch. Somsen, Ch. Fell, and M. Acet, *J. Phys. IV* **11**, Pr8-245 (2001).
- <sup>16</sup>E. Duman, M. Acet, Y. Elerman, A. Elmali, and E. F. Wassermann, *J. Magn. Magn. Mater.* **238**, 11 (2002).
- <sup>17</sup>V. V. Godlevski and K. M. Rabe, *Phys. Rev. B* **63**, 134407 (2001).
- <sup>18</sup>S. Morito, T. Kakeshita, K. Hirata, and K. Otsuka, *Acta Mater.* **46**, 5377 (1998).